

Development of a system for predicting the printed part quality

Ngoc-Hien Tran

Faculty of Mechanical Engineering, University of Transport and Communications

ABSTRACT

3D printing known as additive manufacturing (AM) has been applied for applications in different fields such as aerospace, automotive, biomedical, and energy industries. Currently, with the rapid growth of this technology, 3D printing has gained a very wide acceptance. However, several significant hurdles prevent its wider adoption. One of the most important barriers is the quality of the printed parts, particularly for metals. This research proposes to develop a system for predicting the quality of the part from the manufacturing planning in order to remove the failures before carrying out the real printing process. For accurately predicting quality before manufacturing, consolidation mechanisms used in laser and powder bed based layered manufacturing such as SLM (Selective Laser Melting) must be analyzed. Without an understanding the consolidation mechanisms in each particular case, it will be difficult, if not impossible, to develop a predictive system. AM process for printing metallic parts is characterized by high heat source and fast solidification which lead to large thermal stress. For developing such system, model for predicting the temperature distribution should be generated. From this model, interrelationship between process parameters and temperature distribution should be derived out. Based on that, the deformation can be predicted through calculating residual stress with the result of temperature distribution.

Keywords—Additive manufacturing, Selective laser melting, Quality of the printed part, Prediction system

Date of Submission: 07-10-2022

Date of Acceptance: 18-10-2022

I. INTRODUCTION

Additive manufacturing (AM) technology has been applied widely for applications in different fields. Figure 1 shows the percentage of the industrial sectors using AM such as aerospace, automotive, biomedical, energy industries, and so on.

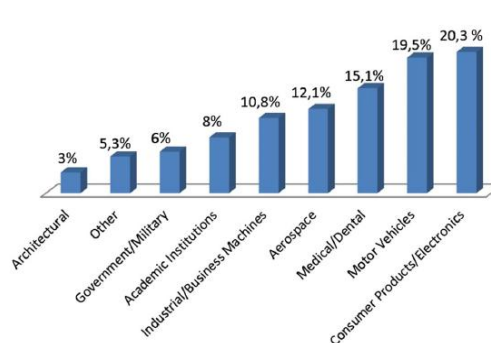


Figure 1. Percentage of the industrial sectors using AM [1, 2]

For fabricating metallic parts, currently, there are a large number of different AM processes using different combinations of stock material form, material delivery, and heat source. Figure 2 shows the AM classification divided into two groups as powder bed-based AM processes and powder injection. In the powder-based processes, metallic powder is spread on the bed before being scanned by the beam or being fed directly to the heat source affected region.

The powder bed processes can be further classified based on whether the stock material gets fully melted, partially melted, or a polymer binder is used for consolidation [3]. The powder bed processes use thermal energy

to selectively fuse areas of a layer of powder using laser or an electron beam as the energy source. When the energy source traces the geometry of an individual layer onto the top surface of the powder bed, the energy from the beam spot is absorbed by the exposed powder causing that powder to melt. With powder fusion getting fully melted such as selective laser melting (SLM), electron beam melting (EBM), and electrographic layered manufacturing these processes use high power energy beams to fully melt the powder particles, which then fuse together to the previous layer(s) when the molten material cools. Another class of powder bed processes use low power lasers to bind powder particles by only melting the surface of the powder particles (called selective laser sintering or SLS) or a binder coating the powder particles. These processes produce green parts that require further post-processing to infiltrate and sinter the parts to make them fully dense [4]. Selective laser melting (SLM) is a powder bed-based AM process to manufacture metallic parts. SLM is the complex process of the interaction between a concentrated laser source and metallic powders.

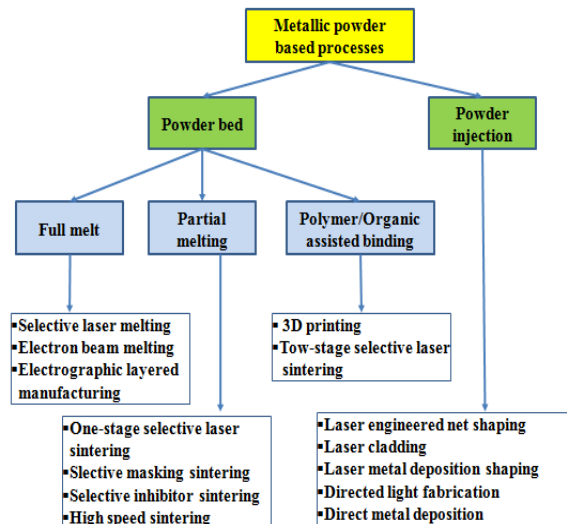


Figure 2. Classification of metallic powder additive manufacturing processes [3]

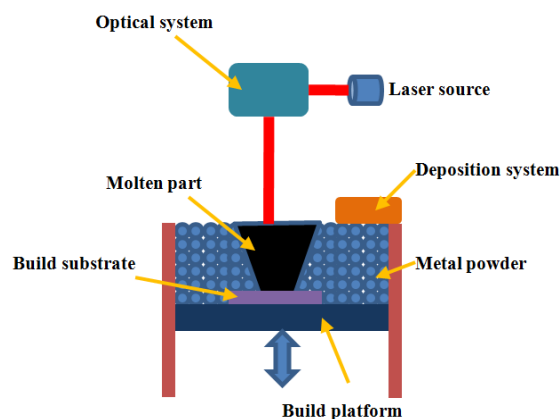


Figure 3. Mechanism of selective laser melting process

Figure 3 shows the mechanism of SLM process. In SLM, a very thin powder layer is distributed and selectively melted by a controlled laser. This procedure is repeated until a complete part is built [5, 6]. The optical system with a set of optical mirrors enables the laser source to direct onto the powder bed surface. The optical system can contain additional elements that allow the melt pool shape and intensity to be monitored. The powder is deposited onto the build area by a deposition system such as scraper or roller system moving over the surface. Before each layer is scanned, this powder container is raised and powder is then pushed across the powder bed by the deposition system. Then, the build platform is lowered by one layer thickness, making the new powder layer on top. Lowering the base plate, depositing powder and scanning of the laser over the powder bed are the three steps that are repeated during the SLM process to produce a 3D part [5].

SLM has been applied widely for manufacturing the metallic parts. However, due to the rapid heating and cooling, several defects usually exist in a SLM part such as the high temperature gradient which generates high thermal stress and leads to part distortion and cracks [7-10]. The high viscosity and surface tension of the

molten powder zone due to the balling effect may result in very poor surface finish. Also, un-melting powder and oxidized particle may also lead to porosity of the manufactured parts [11, 12]. The quality of the final part is decided by powder properties, process parameters and SLM machine characteristics as shown in Figure 4 [5, 13, 14]. For getting the best quality of the printed part, influence factors must be considered such as material properties, machine specifications, printing conditions and process parameters. However, during SLM process, the localized compression and tension caused by the large thermal gradients and fast cooling will increase that lead to the significant residual stresses in SLM parts. Due to existing residual stresses, the localized deformation will result in a loss of part shape as well as other failure of the SLM part [6].

This research presents a predictive system for analyzing the temperature distribution and predicting the deformation of the printed part. The development of a system for predicting the quality of the part from the manufacturing planning in order to remove the failures before carrying out the real printing process is necessary.

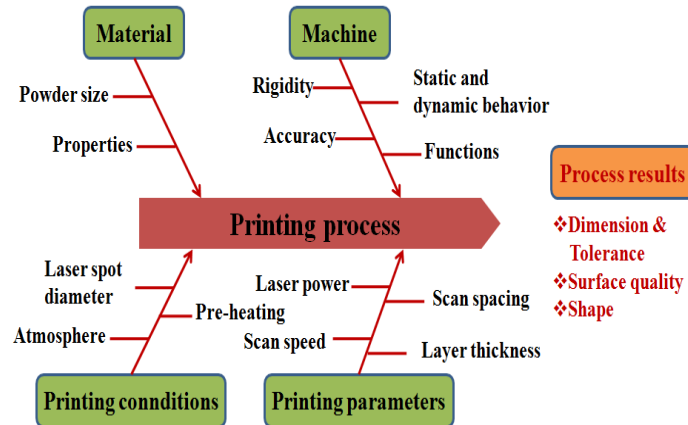


Figure 4. Influence factors affecting the quality of printed part

II. INNOVATION AND CHALLENGES OF AM PROCESS

Currently, with the rapid growth of this technology, there are a large number of 3D printing methods in the market. It is the fact that 3D printing has gained a very wide acceptance over the last decade. With effort to have good connection of the research, innovation and product development with industrial practice, the science and engineering community is gravitating toward an AM solution such as driving out the AM standards. Standards are available for common requirements and generally applicable in AM such as ASTM F2792-12a, ISO 17296-1 and so on.

Due to the lacked any type of standardization for AM, ASTM International was founded committee F42 to develop and maintain standards on AM. In 2013, ASTM and ISO agreed to cooperate on the development of international standards, and devised a fast-track process for ISO to adopt existing ASTM standards, and vice versa. In 2016, specialized material properties standards that include requirements for minimal mechanical properties have been published for Ti6Al4V, Ti6Al4V-ELI, Inconel718 and -625, with more standards underway for CoCrMo, 316L, 15-5PH and 17-4PH steel [5].

In recent years, additive manufacturing (AM) has emerged as a promising manufacturing technique to enable the production of complex engineering structures with high efficiency and accuracy. However, manufacturing of end use parts, particularly on a large scale, introduces new challenges to the advancement of additive technologies. A particular difficulty is ensuring part quality and reproducibility [15].

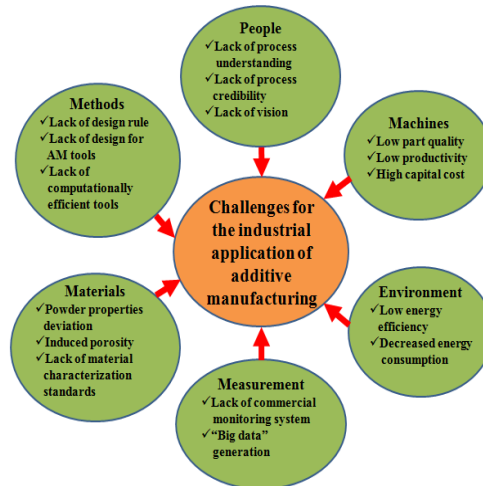


Figure 5. Challenges in additive manufacturing industrial application [3, 16]

Figure 5 shows the challenges for the industrial applications of additive manufacturing in consideration of factors such as materials, machines, measurement, methods, environment as well as people.

Figure 6 shows parameters affecting to the powder properties for AM process. Powder properties themselves include many different aspects such as the particle size distribution and related powder density (bulk and tap density) as well as flow ability, which directly affect the layer generation capabilities. Furthermore, the optical and thermal properties are also affected by these parameters.

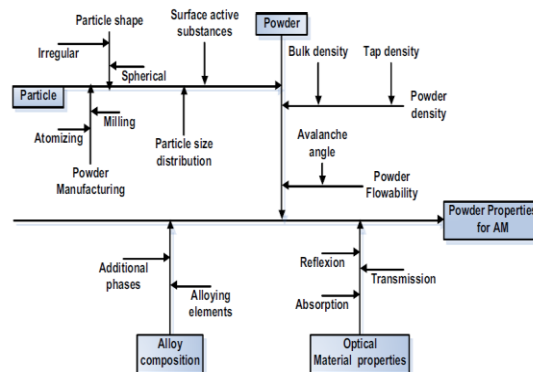


Figure 6. Influencing parameters for metal powder properties [17]

In powder bed based additive manufacturing process, the spatial distribution of the individual powder particles is random. The distribution of particles in the heat affected zone defines the thermo-physical properties of the region being processed by the heat source. So, the distribution of particles plays an important role in heat transfer processes [18].

Currently, there are a limited number of commercial alloys used in AM. In the development of AM, it is important to develop the new alloys to exploit the advantages of AM. Ti-6Al-4V has been by far the most extensively investigated. This can be attributed to the strong business case that can be developed for complex, low production volume titanium parts [19].

Management and sharing data also are challenges in AM field. With the archiving of build data in a database format makes it easier to explore interactions and correlations between factors that are of critical interest to the additive manufacturing community. As the requirement, this work also needs the development of standards and baseline material properties for additively manufactured materials [20].

The widespread adoption of AM is challenged by part quality issues, such as dimensional and form errors, undesired porosity, delamination of layers, as well as poor or undefined material properties [4]. AM process mechanisms present a high level of complexity; the physical mechanisms are still under investigation and a lot of research is undertaken for better comprehension [3].

The AM community also faces the technology challenges in process controls, sensors and models. There is a need for real-time, closed-loop process controls and sensor in order to ensure quality, consistency, and reproducibility across AM machines. Since the properties of AM materials are tied to the immediate past

processing history such as temperature distribution, thermal stress; sensors are being developed to measure melt pool size and shape as well as melt pool and build temperatures. These data in combination with predictive algorithms are needed in order to adjust and control process parameters in real time to ensure quality, consistency, and reliability [19].

Currently, the empirical observations of finished additive parts are used. Then, heuristics are applied to make design, machine parameter, or machine hardware changes in order to reduce variability in subsequent builds as in-process sensing remains uncommon in industrial settings [15].

Among the important factors establishing AM as a sustainable manufacturing process is the ability to control the microstructures and properties of AM products. In most AM processes, rapid solidification and high-temperature phase transformations play primary roles in determining nano- and micro-structures, and consequently the mechanical and other properties of AM products. The qualification of AM parts remains challenging and requires fundamental understanding of processing microstructure–property linkages [21]. It is important to establish correlations between the AM process parameters and the process/part characteristics, to ensure desirable part quality and promote widespread adoption of AM technology. Once the correlations are established, in-process sensing and real-time control of AM process parameters can be done to minimize variations during the AM build process to ensure resulting product quality and production throughput [4].

In powder bed-based AM processes, SLM process requires a high temperature for melting the metallic powders. Due to high temperature and fast cooling, residual stress will be generated in the printed part which leads to part distortion and negatively affect product performance. Part distortion caused by the tensile residual stress not only reduces the part geometrical accuracy but also affects the functional performance of the printed parts. On the other hand, to fix the part distortion of the printed part, the post processing must be carried out that will increase the manufacturing cost [11, 12]. So, the temperature distribution and residual stress fields during the SLM process must be analyzed to keep the quality of the printed parts. In the literature, many researchers have proposed methods for predicting the temperature distribution and residual stress during SLM process. These methods can be classified into three groups. The first group is the simulation method [22]. The second group is the researches which focus on the experimental works [23]. The last group is the comparison of simulation and experimental results [10].

Simulation methods are suitable to predict residual stress and part distortion of the SLM processes. However, these methods are only suitable for analysing the thermal-mechanical model to predict residual stress and distortion of printed part on a small domain [11]. With the real SLM part, it is difficult to predict part distortion due to requiring millions of micro-scale laser scans which will increase the computational ability of the computer hardware even using a very powerful work station [11, 12].

A multi scale approach is highly needed to achieve acceptable accuracy of part distortion and residual stress with low computational cost. Li et al. proposed to divide a SLM process for a practical part into three scales such as micro scale, meso scale and macro scale [12]. With this approach, the temperature history and residual stress fields during the SLM process were predicted. Thermal information has been transferred through micro scale laser scanning, meso scale layer hatching, and macro scale part build-up [11].

In experimental works, an effort to better understand the factors influencing macro scale residual stresses, a destructive surface residual stress measurement technique coupling with a non-destructive volumetric evaluation method were applied [6]. The applications of optical and scanning electron microscopy have been proposed. Residual stresses are measured qualitatively using a novel deflection method and quantitatively using X-ray diffraction [14].

The paper presents a predictive system for analyzing the temperature distribution and predicting the deformation of the printed part. These results are used for determining the optimal process parameters for SLM process and testing on the MetalSys150 - SLM machine.

III. MODEL OF QUALITY ORIENTED PREDICTIVE SYSTEM

The printed part is designed in 3D model using CAD software. This data is transferred to the printing machine for printing process. With the high temperature distribution and fast solidification during printing process, residual stress is generated in the printed part which leads to the deformation of the part. The proposed system enables to predict the deformation of the printed part before printing. For realizing the predictive system, the databases about temperature distribution, residual stress, and deformation from the experimental as well as simulation results must be built. These databases are background for analyzing the influence factors affecting to the quality of the printing process. With results from comprising between the experiment and simulation, the system generates the optimal process parameters in consideration with the quality criteria for the printed part.

3.1. Prediction of temperature distribution

Figure 7 shows the temperature gradient mechanism with deformation of the part in heating and cooling process.

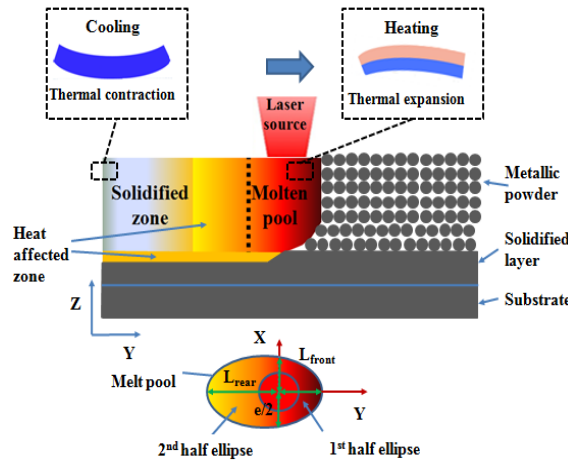


Figure 7. Temperature gradient mechanism (adapted from [24, 25])

When laser source scans on the powder surface, energy is transferred from the top surface to subsurface through various physical changes such as heat transfer, radiation, convection, conduction, fluid flow within the molten pool, melting, evaporation, and chemical reactions. During SLM process, thermal expansion at layers of the printed part happens which lead to the part deformation.

At the top surface of the powder bed, the energy from the beam spot is absorbed by the exposed powder causing that powder to melt. This small molten area is often described as the melt-pool as shown in Figure 10. Individual powder particles are fused together when the melt-pool re-solidifies. After one layer is completed, the build platform is lowered by the prescribed layer thickness, and a new layer of powder from the dispenser platform is swept over the build platform, filling the resulting gap and allowing a new layer to be built [4].

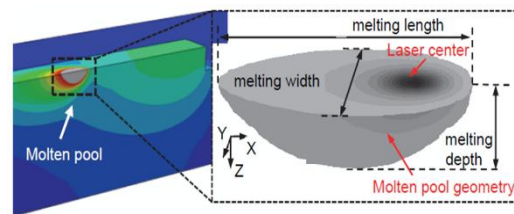


Figure 8. Molten pool geometry [24]

Figure 8 describes the melt pool size in SLM process. A description of temperature values in the molten pool is thus provided by equation as follows, using geometrical features of the melt pool and the maximum temperature T_{max} obtained by finite element simulations [25].

- for $y > 0$ (front semi-ellipse)

$$T = T_m + \frac{1}{2}(T_{max} - T_m) \cdot \left(1 + \cos \left(\pi \left(\frac{x^2}{(e/2)^2} + \frac{y^2}{L_{front}^2} + \frac{z^2}{p^2} \right) \right) \right) \quad (1)$$

- for $y < 0$ (rear semi-ellipse)

$$T = T_m + \frac{1}{2}(T_{max} - T_m) \cdot \left(1 + \cos \left(\pi \left(\frac{x^2}{(e/2)^2} + \frac{y^2}{L_{rear}^2} + \frac{z^2}{p^2} \right) \right) \right) \quad (2)$$

With L_{front} : front part of the melt-pool length; L_{rear} : rear part of the melt-pool length; e : melt-pool width; p : melt-pool depth; T_{max} : maximum temperature (K); T_m : melting temperature (K); and p : melt-pool depth (μm).

In consideration of the heat transfer model due to thermal conductivity, the mathematical model of the heat transfer is as follows [26]:

$$\rho C \frac{\partial T}{\partial t} - \nabla \cdot (k \nabla T) = Q \quad (3)$$

where T is temperature; ρ , C , k are density, thermal capacity, and thermal conductivity factor, respectively. Q is originating or absorbed heat.

Heat-transfer properties of powdered materials (ρ , C , k) differ considerably from those of solid (monolithic) materials, they are identified experimentally and given in Table 1.

Laser impact is determined as a volumetric source of heat, the intensity of which depends on laser impact at various depths of the powder layer. The equation to calculate the laser impact heat is as follows:

$$Q(x, y, z) = Q_0(1 - R_c) \cdot \frac{A_c}{\pi\sigma_x\sigma_y} e^{-\left[\frac{(x-x_0)^2}{2\sigma_x^2} + \frac{(y-y_0)^2}{2\sigma_y^2}\right]} \cdot e^{-A_c z} \quad (4)$$

where Q_0 is the laser emission power; R_c is reflection coefficient; and A_c is absorption coefficient;

$$e^{-\left[\frac{(x-x_0)^2}{2\sigma_x^2} + \frac{(y-y_0)^2}{2\sigma_y^2}\right]} \quad (5)$$

which is the 2D Gauss distribution of emission power over the sample surface in the plane x, y ; $e^{-A_c z}$ is the exponential decay of power over the layer depth of a sample. The following assumptions are to be taken into consideration when implementing the model [26]:

- reflection and absorption coefficients are constant;
- thermal effects of phase transformations are not taken into account;
- the surface of powder layer, along which the laser beam is moved, is parallel to the plane $x-y$ of the system of coordinates;
- the upper plane of the powder layer is smoothed out according to $z=0$, consequently, the effect of power absorption can be expressed as follows: $exp(-A_c \cdot abs(z))$;
- the center of laser beam can be displaced via changing the variables x_0 and y_0 ;

Table 1. Parameters for simulation of temperature distribution of Ti6Al4V

Name	Description	Value
x_0	Path center X-Coordinate	-20 [mm]
y_0	Path center Y-Coordinate	0 [mm]
σ_x	Pulse x standard deviation	0.1 [mm]
σ_y	Pulse y standard deviation	0.1 [mm]
Q_0	Total laser power	180 [W]
R_c	Reflection coefficient	0.05
A_c	Absorption coefficient	100 [1/cm]
L	Product length, width	40 [mm]
L_z	Product thickness	5 [mm]
v	Laser velocity	1500 [mm/s]
C	Thermal capacity	710 [J/(kg*K)]
ρ	Density	4940 [kg/m ³]
k	Thermal conductivity factor	7.5 [W/(m*K)]

Figures from 9 to 15 show the temperature distribution results using COMSOL tool for Ti6Al4V material. For analyzing the temperature distribution along the printing path, the input parameters as shown in Table 1 were used. Figures 9 and 10 show temperature distribution at printing time 0.010667 s and 0.026667 s. With the melting temperature and solidus temperature are 1928 K and 1878 K, respectively, the melt pool length is 1380 μ m as shown in Figure 11.

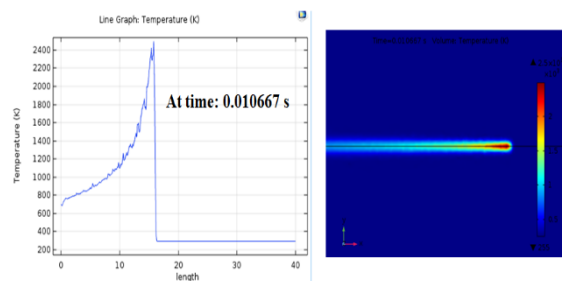


Figure 9. Temperature distribution when printing 1 track at time 0.010667 s

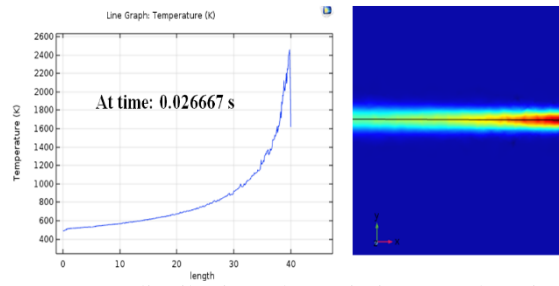


Figure 10. Temperature distribution when printing 1 track at time 0.026667 s

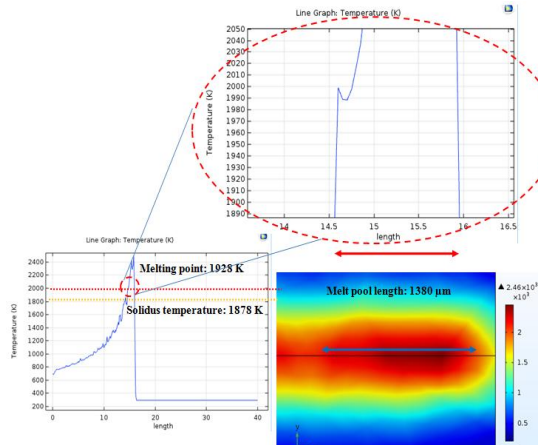


Figure 11. Measurement of melt pool length

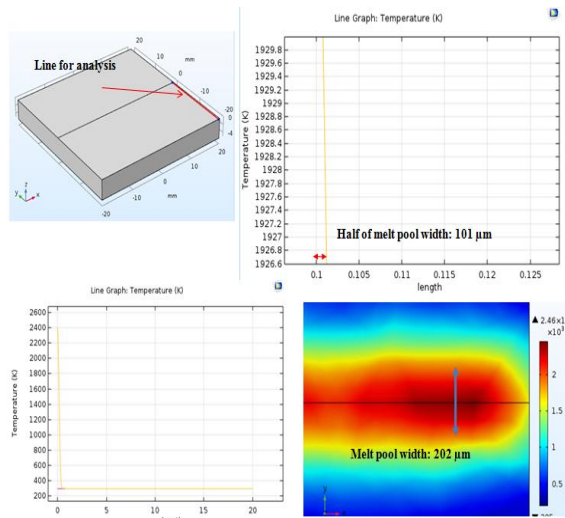


Figure 12. Measurement of melt pool width

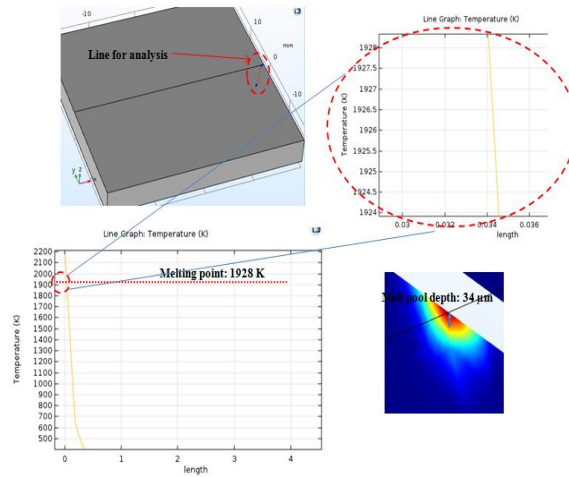


Figure 13. Measurement of melt pool depth

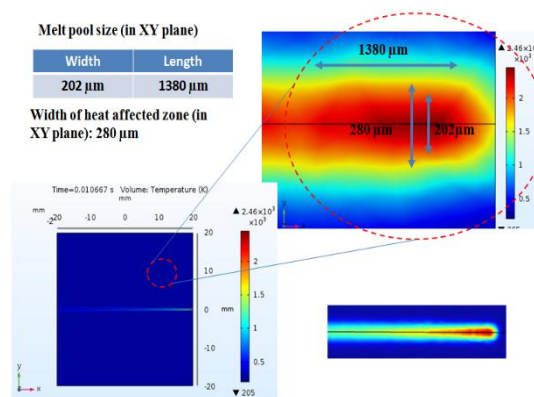


Figure 14. Melt pool size

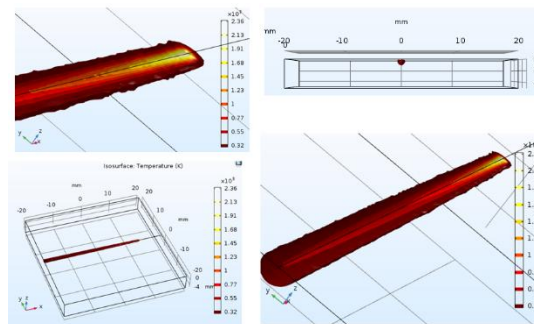


Figure 15. 3D model of melt pool

The melt pool width with 202 μm is determined as shown in Figure 12. The melt pool depth determined as shown in Figure 13 is 34 μm. Summary of measurements for melt pool size and 3D model of the melt pool are shown in Figure 14 and 15, respectively.

3.2. Prediction of residual stress and deformation

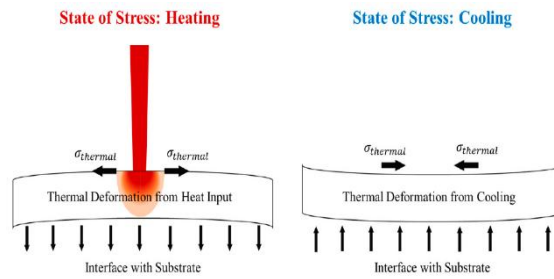


Figure 16. Stress gradients in single layers [26]

In the SLM process, the major source of the residual stresses is the heat cycling as the laser scans across each layer, where previously solidified layers are re-melted and cooled several times at inconsistent levels of heat. Figure 16 shows the stress gradients in single layers. When looking at the stress gradients in a particular single layer of the part during heating, the two most important regions are the top of the layer (exposed to the laser) and the interface between the layer and the previous layer [26].

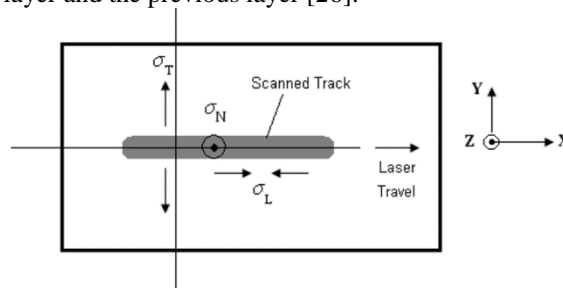


Figure 17. Residual stress classification [27]

Due to thermal expansion, the top of the layer experiences a tensile stress, while the cooler interface has compressive stresses acting on it. Figure 17 shows residual stresses in SLM part. These stresses can be divided into three types as follows [27]:

- Longitudinal stress, σ_L : the component of the residual stress acting parallel to the direction of the laser scanning path. It is given by the X-direction stress component;
 - Transverse stress, σ_T : the component of the residual stress acting perpendicular to the direction of the laser scanning path. It is given by the Y-direction stress component;
 - Normal stress, σ_N : the component of the residual stress acting normal to the surface plane. It is given by the Z-direction stress component. Three stages of this stress during SLM process is described as Figure 18 [28].
- The thermal states are divided into three regions including the melted zone (region I), heat-affected zone (region II), and non-affected zone (region III). During heating, the laser beam irradiates at a specific point, then the temperature of region II falls between the range of t_n (room temperature) and t_p (solidus temperature), the material expands but is restricted by region III.

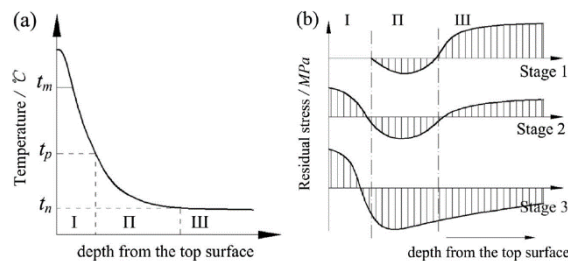


Figure 18. Temperature and residual stress distribution in Z direction [28]

This consequently induces tensile stress in region III and compressive stress in region II. Since the temperature of region I exceeds t_p (melting point), it is converted into a complete plastic state and therefore no residual stress is produced, as illustrated at stage 1. During cooling, the laser beam moves away from the specific point and the temperature immediately decreases. When the temperature of region I is lower than t_p , the material changes from the former complete plastic state into an incomplete plastic state and the volume shrinkage is restricted by region II. Thus, tensile stress is produced in region I and compressive stress in region II increases, as shown at

stage 2. As the temperature drops continuously, region I shrinks further, but is still restricted by region II. This causes tensile stress in region I and compressive stress in region II to further increase, and compressive stress is extended to region III, as illustrated at stage 3 [28].

There are many factors relating to laser beam parameters, material parameters, product properties and process parameters which affect to the residual stress distribution in SLM part. Figure 19 shows the relationship among research fields such as stress and deformation, thermal distribution, and micro-structural organization. The residual stress and deformation of printed part must be considered in relationship with research on temperature distribution as well as micro-structural state of the printed parts [29].

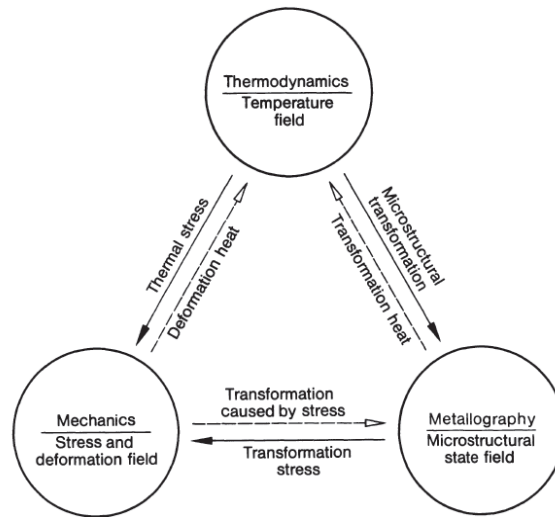


Figure 19. Temperature, stress and deformation, and micro-structural state fields [29]

3.3. Development of the proposed system

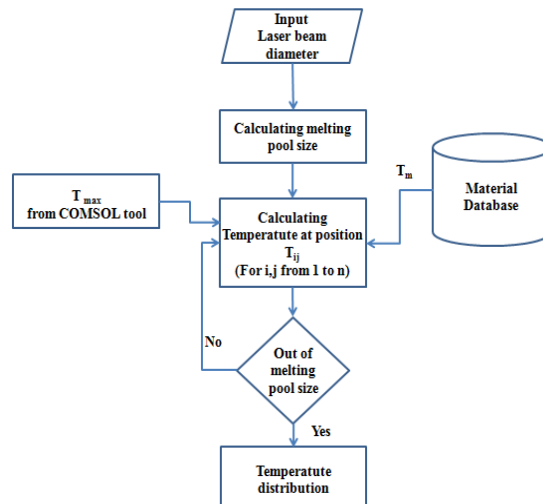


Figure 20. Algorithm for predicting the temperature distribution

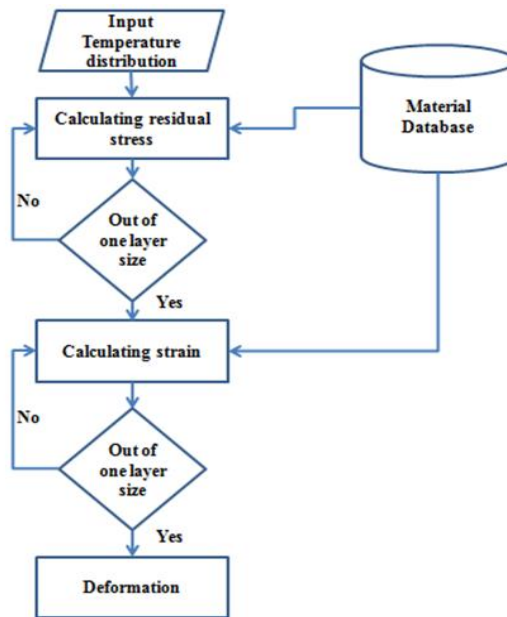


Figure 21. Algorithm for predicting the deformation

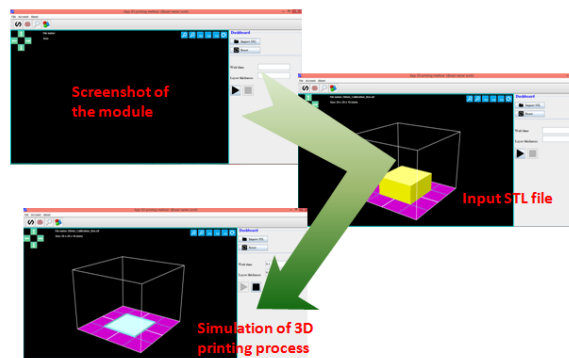


Figure 22. Screenshot of the module for inputting CAD model in STL file

Algorithms for predicting temperature distribution is shown in Figure 20 in which the temperature at any position is predicted according to the material database, melting pool size and using the equations 2 and 3. The stress and strain in SLM part is predicted using the algorithm as shown in Figure 21.

The interface of the predictive system is shown in Figure 22. The 3D-CAD model is inputted in STL file format. The screenshot of the predictive system with three modules is shown in Figure 23. Material information and SLM process parameter are inputted from module #1. Module #2 enables to determine the temperature distribution during SLM process. Then, the temperature information is used for analyzing residual stress and predicting deformation of the part as shown in module #3.

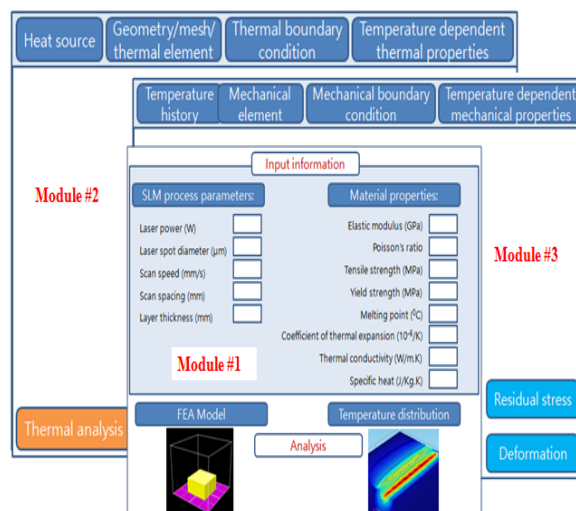


Figure 23. Modules of the predictive system

IV. CONCLUSIONS

Additive manufacturing technology is more and more applied to many fields. The innovation and development of this technology enable to have not only the prototype products but also have the functional parts for the real applications. However, there are many challenges for the industrial applications of additive manufacturing in consideration of the quality of the printed parts, evaluation standards, development of the material science, as well as micro structural analysis. Further challenges are the data management and control technology for in-process sensing to ensure the quality of the printed part during the AM process. The aim of this research is to develop a system for predicting the printed part quality to remove the failure before carrying out the real printing process. For predicting the quality of the SLM part, the temperature distribution and residual stress are predicted. Then, the part deformation due to the residual stress is determined. For developing the prototype system, three modules are established which include the input module with the material information and SLM process parameter; the module for predicting the temperature distribution; and the module for analyzing residual stress and predicting deformation of the part. The database of the developed predictive system is built according to AM standards in terms of materials, printing methods and requirements of the printed parts. The system enables to analysis the SLM process and to remove the failures before carrying out the real printing process.

REFERENCES

- [1] Bikas H., Stavropoulos P., Chryssolouris G. (2016), Additive manufacturing methods and modelling approaches: a critical review, *Int J Adv Manuf Technol*, 83:389–405.
- [2] Wohlers T.T. (2012) Wohlers report 2012: additive manufacturing and 3D printing state of the industry: annual worldwide progress report. Fort Collins, Wohlers Associates.
- [3] Salonitis K. (2016) Energy efficiency of metallic powder bed additive manufacturing processes, pp. 1-29. In *Handbook of Sustainability in Additive Manufacturing*, Muthu S.S., Savalani M.M. (eds.), Springer.
- [4] Mahesh M., Brandon L., Alkan D., Shaw F., Shawn M., Ronnie F. (2015), Measurement science needs for real-time control of additive manufacturing powder bed fusion processes, National Institute of Standards and Technology, U.S. Department of Commerce.
- [5] Vrancken B. (2016), Study of residual stresses in selective laser melting, Ph.D Dissertation.
- [6] Wu A.S., Brown D.W.B., Kumar M., Gallegos G.F., King W.E. (2014), An experimental investigation into additive manufacturing induced residual stresses in 316l stainless steel, *Metall and Mat Trans A* 45 6260.
- [7] Kundakcioglu E., Lazoglu I., Rawal S. (2016), Transient thermal modeling of laser-based additive manufacturing for 3D freeform structures, *Int J Adv Manuf Technol*, 85 493.
- [8] Cheng B., Shrestha S., Chou K. (2016), Stress and deformation evaluations of scanning strategy effect in selective laser melting, *Additive Manufacturing*, 12 240.
- [9] Saprykin A.A., Ibragimov E.A., Babakova E.V. (2016), Modeling the temperature fields of copper powder melting in the process of selective laser melting, *IOP Conf. Series: Materials Science and Engineering* 142 012061.
- [10] Zaeh M.F, Branner G. (2010), Investigations on residual stresses and deformations in selective laser melting, *Prod Eng Res Devel* 4 35.
- [11] Li C., Liu J.F., Guo Y.B. (2016), Efficient multiscale prediction of cantilever distortion by selective laser melting, *Annual International Solid Freeform Fabrication Symposium*.
- [12] Li C., Fu C.H, Guo Y.B. (2016), A multiscale modeling approach for fast prediction of part distortion in selective laser melting, *J Materials Processing Technology* 229 703.
- [13] Van Gestel C. (2015), Study of physical phenomena of selective laser melting towards increased productivity, Ph.D Dissertation.
- [14] Vrancken B., Wauthe R., Kruth J.P., Van Humbeeck J. (2013), Study of the influence of material properties on residual stress in selective laser melting, *Proceedings of the Solid Freeform Fabrication Symposium*, pp: 393-407.

- [15] Thomas G.S., Scott A.G. (2016), In-process sensing in selective laser melting (SLM) additive manufacturing, *Spears and Gold Integrating Materials and Manufacturing Innovation* 5:2, pp.1-25
- [16] Schoinochoritis B., Chantzis D., Salonitis K. (2015) Simulation of metallic powder bed additive manufacturing processes with the finite element method: a critical review, *Proc Instit Mech Eng Part B J Eng Manuf*.
- [17] Spierings A.B., Voegtlin M., Bauer T., Wegener K. (2016), Powder flowability characterisation methodology for powder-bed-based metal additive manufacturing, *Prog Addit Manuf* 1:9–20.
- [18] Jonas Z., Simon V., Hans W.M., Mustafa M. (2017), Influence of powder bed characteristics on material quality in additive manufacturing, *BHM* 162 (5): 192–198.
- [19] William E.F. (2014), Metal additive manufacturing: A review, *JMEPEG* 23:1917–1928.
- [20] Tracie P. (2017), Database development for additive manufacturing, *Prog Addit Manuf* 2:11–18.
- [21] Zaeem M.A., Clarke A.J. (2016), Rapid solidification and phase transformations in additive manufactured materials, *JOM* 68 (3) 928-929.
- [22] Wischeropp T.M, Salazar R., Herzog D., Emmelmann C. (2015), Simulation of the effect of different laser beam intensity profiles on heat distribution in selective laser melting, *Lasers in Manufacturing Conference*.
- [23] Casavola C., Campanelli S.L., Pappalettere C. (2008), Experimental analysis of residual stresses in the selective laser melting process, *Proceedings of the International Congress and Exposition*.
- [24] Fu C.H., Guo Y.B. (2014), 3-Dimensional finite element modeling of selective laser melting Ti-6Al-4V alloy, *Proceedings of the 25th Annual International Solid Freeform Fabrication Symposium*, pp.1129-1144.
- [25] Peyre P., Aubry P., Fabbro R., Neveu R., Longuet A. (2008), Analytical and numerical modelling of the direct metal deposition laser process, *J Physics D: Applied Physics* 41.
- [26] Albert E.P., Sherri L.M., Phillip A.F. (2017), Overhanging features and the SLM/DMLS residual stresses problem: Review and future research need, *Technologies*, 5 (15).
- [27] Ibiye A. R. (2012), Investigation of residual stresses in the laser melting of metal powders in additive layer manufacturing, PhD Dissertation.
- [28] Liu Y., Yang Y., Wang D. (2016), A study on the residual stress during selective laser melting (SLM) of metallic powder, *Int J Adv Manuf Technol*.
- [29] Radaj D. (1992), *Heat Effects of Welding: Temperature Field, Residual Stress, Distortion*, Springer.